





Sustainable Energy Solution for Mobile Robotics: Modeling and Power Management

Bilal Khan, Muhammad Arif, Shaista Afridi, Amir Naveed, Muhammad Sadiq, Mahad Aurangzeb

University of Engineering and Technology, Peshawar

*Correspondence: bskuet@gmail.com, arif.khattak@uetpeshawar.edu.pk

Citation | Khan. B, Arif. M, Afridi. S, Naveed. A, Sadiq. M, Aurangzeb. M, "Sustainable Energy Solution for Mobile Robotics: Modeling and Power Management", IJIST, Vol. 7 Issue. 1 pp 301-312, Feb 2025

DOI | https://doi.org/10.33411/ijist/202571301312

Received | Jan 16, 2025 Revised | Feb 12, 2025 Accepted | Feb 13, 2025 Published | Feb 14, 2025

robotics is increasingly addressing inefficiencies in diverse applications, including healthcare, mining, and defense. This research focuses on energy optimization for a Two-Wheel Mobile Robot (TWMR) using a novel framework that analyzes componentlevel power consumption and evaluates battery performance. Simulations conducted in Gazebo Classic 11, powered by ROS (Noetic), assessed the TWMR's battery discharge rates across different configurations. Results identified the LiDAR sensor as the primary power consumer, with a 300mAh battery significantly extending operational duration (65.83 seconds) compared to a 100mAh battery (21.41 seconds). The study also examined how component integration impacts energy usage, providing valuable insights for future robotic system designs. These findings highlight the critical role of battery size in optimizing energy efficiency and ensuring the prolonged functionality of robotic systems in practical applications.

Keywords: TWMR, Robotics, Gazebo, Battery Size, Energy Optimization





























INFOBASE INDEX



Introduction:

In the current technology-driven world, robots have found applications in almost every facet of life. The massive demand for production prompts the implementation of innovative technologies to fulfill industrial requirements. Automation discussed as a replacement for manual labor, has encountered the drawbacks of human labor, such as errors and nonavailability, in getting tasks accomplished with higher efficiency and accuracy. Many tasks which were hitherto either wholly or partially undertaken by humans are now done by robots. This facility comes with several advantages, not least of which are cost-effectiveness, safety, and ability to operate continuously: a major plus for reliability. They can operate 24x7 without breaks. The use of robots has applications in many diverse fields. In mining, they are engaged in exploration and extraction. They help in surgeries, rehabilitation, and the care of patients in the medical field. It helps provide precision and consistency that brings about better results for patients. Robots are also applied in the defense sector where robots are deployed for surveillance, and bomb disposal among other critical operations. In their integration into various sectors, robots always try to upgrade productivity, safety, and efficiency. The role of robots in daily life and industrial applications is only going to get bigger as technology evolves further [1][2]. For example, rescue robots [3] save human lives by providing useful environmental information to the rescue team during their mission in scenarios such as natural disasters, chemical incidents, structural emergencies, and explosive detection. Swarm robotics pertains to systems comprising vast numbers of existing robots where the hardware tends to be homogeneous, inspired by observations of the group behaviors of insects, ants, and bees [4]. In the realm of robotics, we've encountered various challenges, from design flaws to hardware quality, but the central issue remains the robot's power dilemma, driven by the critical role of its energy system.

One of the primary challenges in robotics is how efficiently to manage its power [5]; this has been bounded by a battery's weight and performance. But heavy batteries not only limit the mobility of any robot but also increase its operational cost, hence energy efficiency is of prime importance. With the intensifying usage of robots in every diversified application—from industries to daily life—the requirement for an effective management system related to their batteries is also increasing [6].

The researchers [7] have placed much effort into better-performance batteries in several ways. For instance, lightweight batteries like lithium polymer "Li-Po "due to their high capacity and convenient application on drones since they provide extended operation time [8][9]. In addition, trajectory planning, control systems, standby modes, and Mechanical design [10][11][12] all aim at decreasing energy consumption and enhancing the overall efficiency. Researchers [13][14], and Rizaldy et al., [15], have performed comparative studies on various types of batteries, such as lead acid, NiMH, and Li-Po, in terms of factors such as cost, weight, and discharge rate.

For battery optimization, some researchers have focused on path motion planning for mobile robots, implementing numerous energy-efficient approaches across various robotic domains, including industrial robots [16], humanoid robots [17], space manipulators [18], soccer robots [19], rover robots [20], and bio-robots for cell manipulation [21]. The design of effective path planning aims to enable robots to perform tasks using minimal energy [22]. Energy constraints were taken into account in addressing multiple sensor coverage issues in a study [23]. In our case, we aim to focus on battery optimization for a Two-Wheeled Mobile Robot (TWMR).

This paper presents a strategy for optimizing power consumption in a Two-Wheeled Mobile Robot (TWMR) through simulation. By examining the power usage of each robot component, our approach aims to refine battery efficiency. We will utilize the Gazebo ROS environment for our simulations to implement and evaluate this strategy. In our simulation, we



calculated the voltage, current, and active time for each component of the Two-Wheeled Mobile Robot (TWMR). This data helps us fine-tune the power optimization strategy to enhance battery efficiency.

Objective:

The objectives of this research are:

- To Analyze the power consumption of the robot's components to optimize battery usage and minimize power drain.
- To consider different battery parameters such as weight, size, shape, and battery type to ensure they meet the specific requirements of the robot.

Novelty:

The novelty of this research lies in its integrated framework for optimizing energy management in robotic systems. By conducting a comprehensive analysis of the power consumption of individual components and evaluating key battery parameters, such as weight, size, shape, and type. This study aims to refine battery selection processes and improve overall power efficiency. This approach offers a tailored methodology for selecting the most suitable battery, minimizing power drain, and enhancing the operational performance and autonomy of robotic systems. Furthermore, the incorporation of power optimization algorithms or the potential integration of energy harvesting techniques represents a novel contribution to advancing energy efficiency in mobile robotics.

Methodology:

This research took place in a computer environment running Linux version 20.04, and we utilized the power of ROS (Robot Operating System) version NOETIC to control our robot. Custom ROS nodes were developed and used as we recorded and saved the data to make algorithms for our project. The flow diagram of the methodology is shown in Figure 1. We utilized Gazebo Classic 11, a simulated environment that allows us to study how TWMR (Turtle Bot 3) manages power in a controlled digital setting. However, for robot movement, its motors are turned ON manually each time to check the power consumption. We obtained insightful results using the above-mentioned software and robot operating system.

In this research, we established a controlled software environment to facilitate the operational tasks of a robotic system. By implementing a series of programmed commands, we arranged various tasks for the TWMR and enabled its movement along a predefined trajectory. Throughout the experimental process, we calculated the battery's discharge rate, current, and voltage across different scenarios.

This research encompassed the determination of the battery discharge rate for individual components, including the microcontroller, LiDAR sensor, and Camera. Furthermore, we evaluated the battery performance in configurations involving a solo robot not equipped or connected with both camera and LiDAR, as well as a fully loaded robot carrying the additional weight of connected camera and LiDAR systems.

Initially, we deactivated the LiDAR and Camera functionalities to isolate the robot's core operations. During this phase, we recorded the battery's active time for the microcontroller and wheels, individually assessing their impact on overall power consumption. Subsequently, we initiated simulations with the LiDAR and Camera activated separately, allowing us to calculate the battery's active time of both components separately with a robot.

In the final stages of our experimentation, we disconnected both the LiDAR and Camera systems, observing the battery's active time for the solo robot configuration. Finally, we reconnected the LiDAR and Camera to the fully loaded robot and estimated the battery active time of the fully loaded robot.



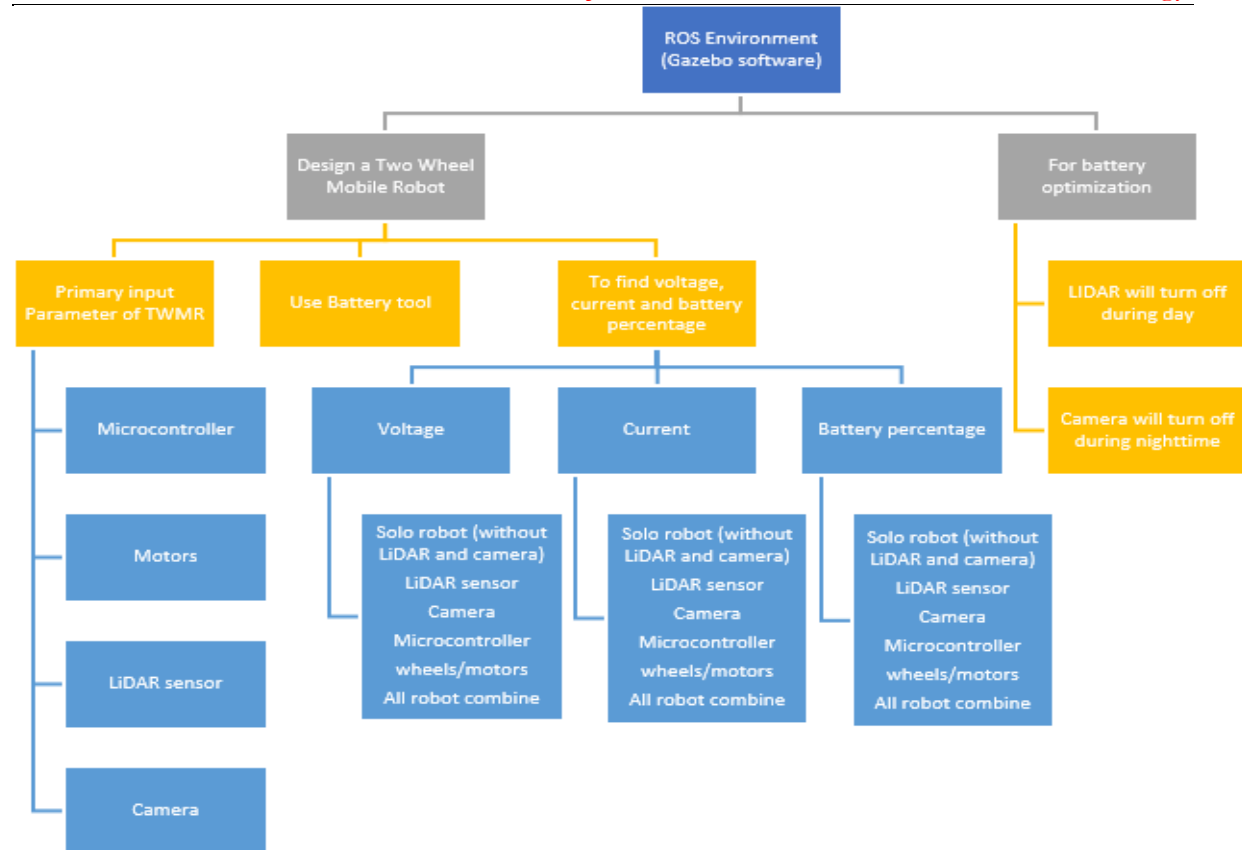


Figure 1. Study Flow Chart

Robot Specifications:

In our simulation, we used a TWMR as mentioned in Figure 2 named Turtle Bot 3, a 2-wheeled mobile robot having 2 DC motors, a 66mm diameter of 2 wheels, a wheel caster, and a Raspberry Pi as a microcontroller. A Turtle bot is assumed to move in any direction along a path in an environment created in software.

A TWMR is equipped with RP LIDAR 12mm and a D455 camera for performance. Powering a robot, we utilized two LiPo batteries – the first, a compact 25V, 100mAh, weighing a mere 0.0125kg, and the second, a more substantial 25V, 300mAh, with a weight of 0.0375kg. These power sources sustain the TurtleBot 3's journey through our research's digital landscapes, advancing the limits of simulated exploration.

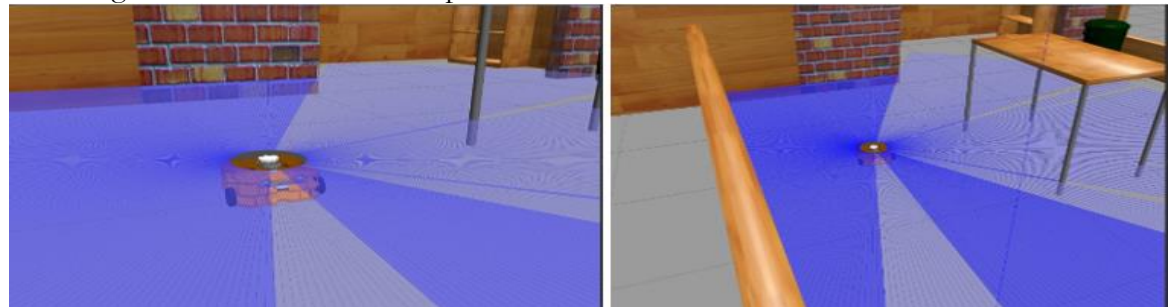


Figure 2. Two-wheeled mobile robot TWMR 3D multibody model in the Gazebo environment

Movement of Robot:

For our TWMR, we selected standard wheels that followed two key principles:

• The front wheels were evenly spaced and remained stable, preventing lateral wobbling, while the rear wheel rotated smoothly without causing unwanted sliding.



• The front wheels moved strictly forward and backward, whereas the rear wheel moved freely.



Figure 3. Two-wheeled mobile robot TWMR in the Gazebo environment.

The rover's front wheels as mentioned in Figure 3 were controlled by actuators, while the idler wheel moved passively, following the rover's overall motion without adding any extra speed limits. We positioned the frame's starting point at the middle of the line connecting the two fixed wheels, with an axis running along this line. This setup allows for three types of movements: straight-forward motion when both front wheels spin at the same speed, rotation around the center when they spin in opposite directions at equal speeds, and rotation around one wheel when the other isn't moving. However, there's no sideways movement, known as singularity. The castor wheel helps overcome any issues caused by slight differences in wheel speeds or variations in ground level. When the front wheels move independently, the rover moves in straight lines or turns, depending on which wheel spins slower. The rover needs to be rotated around a point on the axis between the two wheels to move it in the circle, called the instantaneous curve center. Robots can use various methods to move on land, like walking, jumping, or sliding, but wheels are the most common choice due to their simplicity and efficiency on flat surfaces. The wheels play a crucial role in the rover's movement, so it's essential to choose and arrange them carefully.

Results and Discussion:

In this study, we utilized key input parameters, including the robot's component configurations such as the microcontroller, wheels/motors, LiDAR sensor, and camera along with the corresponding power consumption values for each component. Additionally, battery parameters like discharge rate percentage, current, and voltage were measured across different operational scenarios.

The procedures applied to obtain the results involved a series of controlled experiments within a simulated environment. The robot was tested in various configurations, starting with the core system (microcontroller and wheels) alone, followed by configurations where the LiDAR and Camera systems were activated separately, and finally with both systems reconnected to assess the performance of a fully loaded robot.

To examine the effects of battery variations, we tested two types: a 100mAh battery weighing 0.0125kg and a 300mAh battery weighing 0.0375kg. This comparative analysis aimed to uncover how different battery capacities influence the energy usage of the simulated robot, with findings to be detailed further in subsequent sections, providing insights into battery performance and its implications for robotic operations.

Parameters of Simulation:



In our analysis of battery consumption, we identified four key parameters: voltage, current, battery percentage, and the active time of individual loads or components. Across six distinct scenarios, we evaluated consumption for the controller, motor wheels, and the entire robot under varying conditions—specifically, with LiDAR, with a camera, without LiDAR and camera, and a comprehensive assessment of the fully loaded robot. The subsequent sections delve into an exhaustive analysis of these parameters and outcomes, providing invaluable insights into the nuances of power consumption across various aspects of the simulated robotic system.

Power Consumption at 2.5Wh Battery:

Initially, we analyzed the 100mAh battery to observe its performance., The plots show the relationship between the time (on the x-axis) and the voltage, current, and battery percentage (on the y-axis) for the different components of the robot. The components are represented by different colored lines.

Voltage:

The data presented in Figure 4 illustrates the voltage levels and active times of various robot components, including Solo (without LiDAR and camera), LiDAR, Camera, all robot, Controller, and Wheels, while using a 100mAh, 25V battery. Notably, a trend emerges where components with longer active times tend to exhibit lower voltage consumption. Specifically, the Solo component was active for 44.233 seconds, LiDAR for 24.217 seconds, Camera for 30.125 seconds, All-robot for 21.419 seconds, Controller for 124.409 seconds (the longest active time among all components), and Wheels for 55.357 seconds. This data provides valuable insights into the relationship between active time and voltage consumption across various components of the robot system.

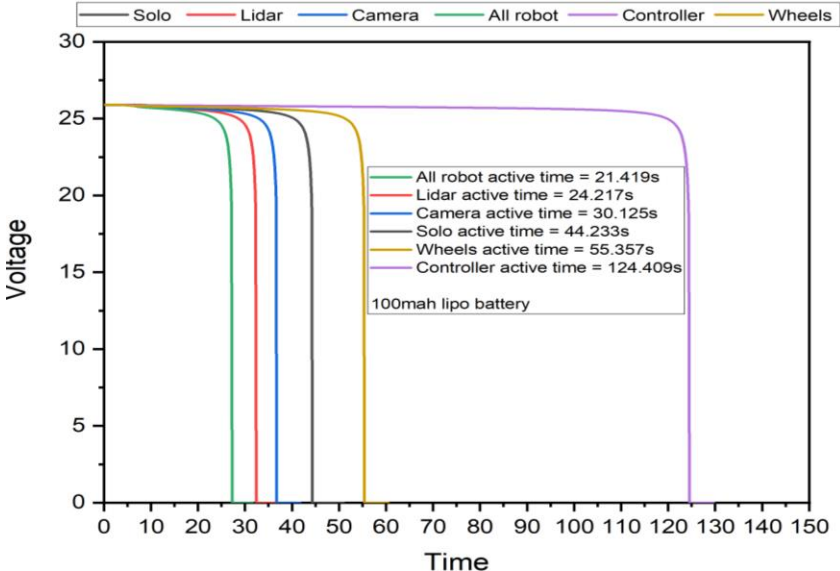


Figure 4. Analyzing the Performance of a Battery: Voltage Degradation Over Time (measured in volts, with time typically recorded in seconds, to observe how the battery's voltage output decreases as it discharges during use or under load conditions)

Current:

The graph presented in Figure 5 illustrates the power consumption or usage of various robot components over a 140-second timeframe. Each component's activity duration is highlighted:

- Solo robot without LiDAR and camera: Active for approximately 44.233s, potentially representing the primary computing unit.
- LiDAR: Active for approximately 24.217s, utilized for navigation and mapping.

- **Camera:** Active for approximately 30.125s, used for visual sensing.
- **Controller:** Active for approximately 124.409s, likely managing component operations.
- Wheels: Active for approximately 55.357s, indicating power usage of the robot's wheels.
- All robots (loaded with camera and LiDAR): Active for approximately 21.419s, illustrating overall power consumption. Notably, a correlation between active time and current is observed, suggesting that longer activity durations correspond to lower current usage.

These insights from the graphs provide a comprehensive understanding of power utilization across various robot components, helping to assess energy efficiency and overall performance.

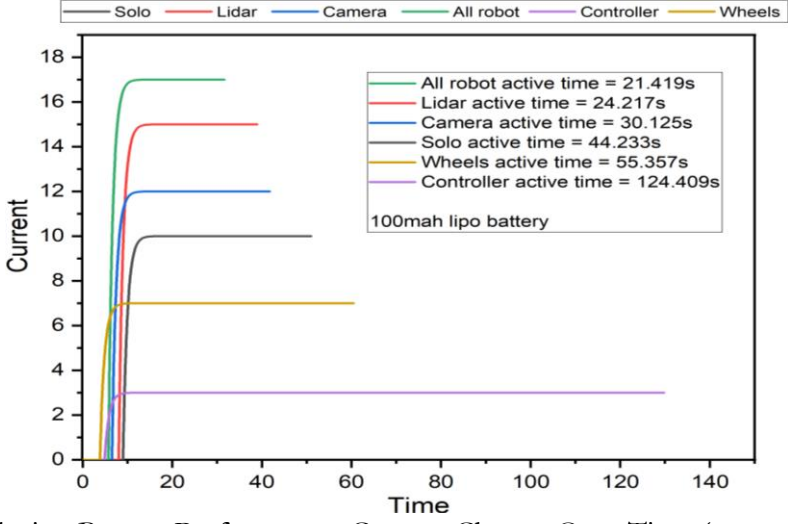


Figure 5. Analyzing Battery Performance: Current Change Over Time (measured in amperes, with time in seconds, to track the battery's current output during discharge or load)

Battery Percentage:

The plot shown in Figure 6 illustrates the correlation between time (x-axis) and the percentage of remaining battery (y-axis) for various robot components, with each component represented by a distinct colored line. Notably, as active time increased, the percentage of battery remaining decreased across all components. The "All robot" line depicts the cumulative battery usage of all components, exhibiting the highest battery consumption and indicating approximately 21 seconds of operation before battery depletion. Conversely, the controller exhibits the lowest battery usage, lasting approximately 125 seconds, suggesting comparatively shorter operational time.

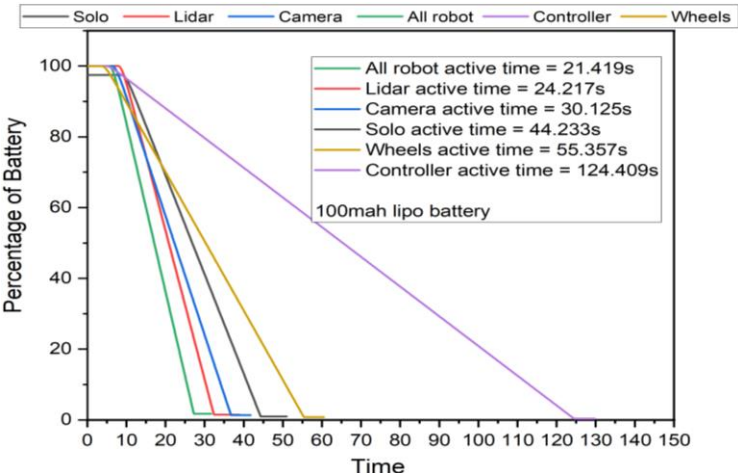


Figure 6. Analyzing Battery Performance: Battery Percentage (%) Over Time (measured in %, with time in seconds, to track the battery's charge level during discharge)



Power Consumption at 7.5Wh Battery Voltage:

Figure 7 shows the active time of each component with voltage, representing the duration of power consumption. The length of the horizontal line for each component indicates its active time. The graph depicts voltage on the y-axis and time on the x-axis, utilizing a 25V, 300mAh battery. Notably, the controller exhibits lower voltage usage and an extended active time of 356 seconds. Moreover, the wheels also consume less voltage and maintain a substantial active duration, surpassing other components. Conversely, the fully loaded robot necessitates the highest voltage and exhibits the shortest active time, recorded at 66 seconds. This data underscores the varying power requirements and operational durations of different components, providing insights crucial for optimizing performance and energy efficiency.

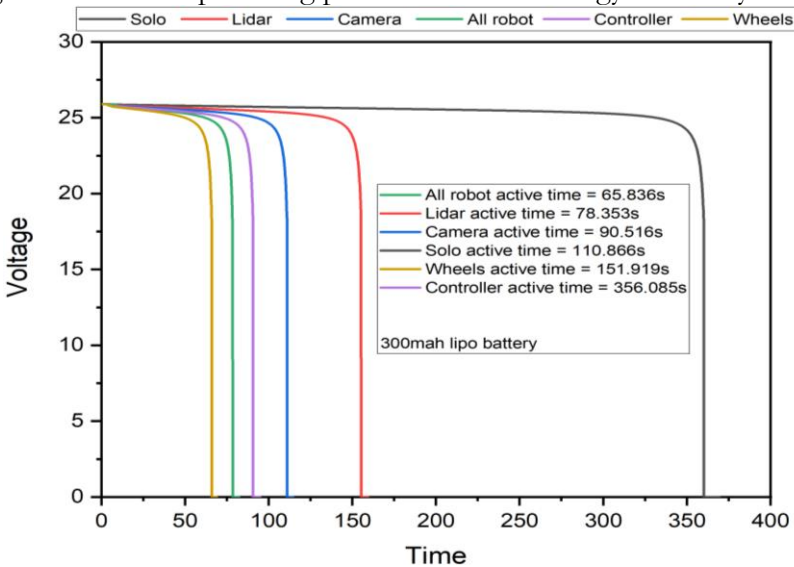


Figure 7. Analyzing the Performance of a Battery: Voltage Degradation Over Time (measured in volts, with time typically recorded in seconds, to observe how the battery's voltage output decreases as it discharges during use or under load conditions)

Current:

Figure 8 illustrates the active time of each component, representing the duration during which power consumption occurred, with the length of the horizontal line indicating this active time. Spanning a measurement period of 400 seconds, the graph showcases the power consumption or usage of various robot components. Specifically:

- The Solo robot without LiDAR and camera was active for approximately 110.866s, potentially serving as the primary computing unit.
- LiDAR, utilized for robot navigation and mapping, remained active for approximately 78.353s.
- The Camera component, facilitating visual sensing, was active for approximately 90.516s.
- The Controller, managing the operation of different components, exhibited the longest active time at approximately 356.085s.
- Wheels, representing the power usage of the robot's wheels, remained active for approximately 151.919s.
- The "All robot" scenario, loaded with both camera and LiDAR, showed an active time of approximately 65.836s.

This data aids in understanding the energy consumption of various components and identifying potential areas for power optimization within the robotic system.

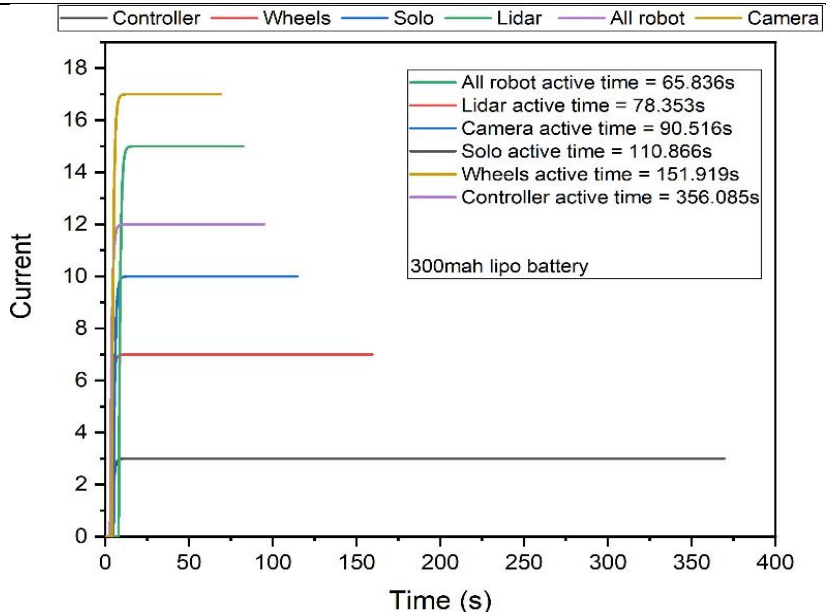


Figure 8. Analyzing Battery Performance: Current Change Over Time (measured in amperes, with time in seconds, to track the battery's current output during discharge or load)

Battery Percentage:

Figure 9 shows the battery usage percentage for various robot components, along with their corresponding active times during operation. The graph includes components such as the controller, wheels, & "solo" (robot without LiDAR and camera), LiDAR, and camera, along with the total active time for the entire robot and the total battery capacity(300mAh). The controller exhibited the lowest battery usage with the highest active time of 356.085s compared to the other components, while the fully loaded robot consumed more battery with the shortest active time. The remaining components also demonstrate varying levels of battery usage and active time, as depicted in the graph. Overall, this graph offers valuable insights into the battery power consumption of each robot component and their corresponding active durations, providing essential data for optimizing power usage and enhancing overall performance.

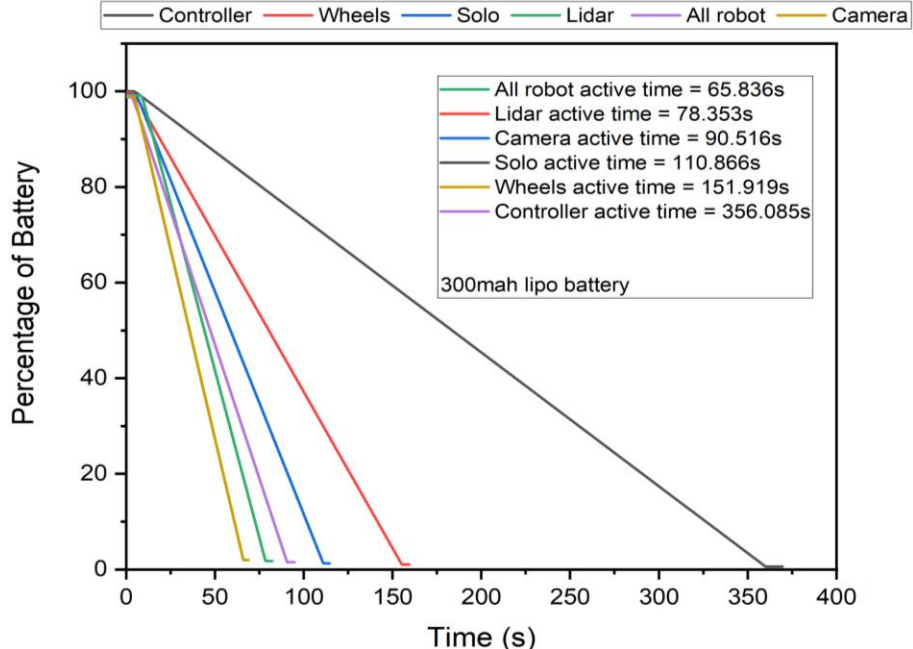


Figure 9. Analyzing Battery Performance: Battery Percentage (%) Over Time (measured in %, with time in seconds, to track the battery's charge level during discharge)



Power Profile for Each Component:

Component	Average Power (W)	Peak Power (W)
Solo Robot	18.6	37.2
LiDAR	13.2	26.4
Camera	15.2	30.4
Controller	60.0	120.0
Wheels	25.6	51.2
All Robot	11.1	22.2
(Camera+LiDAR)		

Comparison with Existing Literature:

Patil, M. [4], et al. proposed battery consumption in the percentage of different components of a rover robot, but in this paper the simulation of essential components such as LiDAR, camera, microcontroller, and motors were utilized to analyze their battery power consumption, monitoring variables like the voltage, current, and battery percentage over time to ascertain the duration of the simulated robot's activity.

Conclusion:

In our preceding chapters, we meticulously scrutinized graphs and numerical data to gain insight into our robot's power consumption patterns. Two pivotal findings emerged from our analysis:

- The current study revealed that the LIDAR sensor emerges as the predominant power consumer within our robot. Its substantial energy demand significantly influences the overall power requirements of our robotic system.
- The comparative study of two battery options—100mAh and 300mAh—unveiled a notable difference in the duration of robot activity. While the 100mAh battery sustained operations for approximately 21.41 seconds, the 300mAh counterpart remarkably extended this duration to 65.83 seconds—more than three times longer than anticipated. Intriguingly, despite its lighter weight, the 100mAh battery did not demonstrate comparable longevity.

The findings indicate that the size of the battery plays a crucial role in how long the robot can operate, more so than just its weight. The research showed that larger batteries result in longer runtimes, allowing the robot to function for extended periods. This highlights the importance of battery size in ensuring smooth robot operation.

The Strategy We Followed:

- In our observations, the LIDAR sensor stands out as the major contributor to energy consumption. To optimize power usage, during daylight, we plan to deactivate the LIDAR and activate the camera since both serve similar functions. However, at night, the camera's performance can be affected by car headlights and low light in certain areas.
- Additionally, when the robot's energy level decreases, a strategic move is to disable the LIDAR temporarily and shift to using the camera. This adaptive approach aims for better optimization under varying energy conditions.

Practical Implication:

This research provides practical insights for optimizing mobile robotic systems, particularly Two-Wheel Mobile Robots (TWMRs). It offers a framework for selecting the right battery size and capacity to maximize runtime while identifying high-energy-consuming components, such as LiDAR sensors, to improve power management. Extending operational time benefits critical applications like rescue, surveillance, and industrial tasks. The use of simulation environments like ROS and Gazebo reduces development costs by minimizing reliance on physical prototypes. Furthermore, the findings are adaptable to various industries, including healthcare, agriculture, and logistics, making the research broadly applicable.



Acknowledgments:

We would like to express our sincere gratitude to the U.S.-Pakistan Center for Advanced Studies in Energy, University of Engineering and Technology, Peshawar, Pakistan, for their invaluable support throughout this research. Our deepest appreciation goes to Dr Mohammad Arif Khattak whose expertise and guidance greatly contributed to this study. We also thank our colleagues and participants for their cooperation and insights, which were instrumental in shaping our findings.

References:

- [1] D. S. Muszyńska Magdalena, Andrzej Burghardt, Krzysztof Kurc, "MONITORING THE PARAMETERS OF THE ROBOT-OPERATED QUALITY CONTROL PROCESS," *Adv. Sci. Technol. Res. J.*, vol. 11, no. 1, pp. 232–236, 2017, doi: 10.12913/22998624/68466.
- [2] M. C. Cafolla Daniele, "An experimental validation of a novel humanoid torso," *Rob. Auton. Syst.*, vol. 91, pp. 299–313, 2017, doi: https://doi.org/10.1016/j.robot.2017.02.005.
- [3] P. S. and J. Suthakorn, "Battery management for rescue robot operation," *IEEE Int. Conf. Robot. Biomimetics (ROBIO), Qingdao, China*, pp. 1227–1232, 2016, [Online]. Available: https://ieeexplore.ieee.org/abstract/document/7866493
- [4] S. P. and T. S. M. Patil, T. Abukhalil, "UB robot swarm—Design, implementation, and power management," *12th IEEE Int. Conf. Control Autom. (ICCA), Kathmandu, Nepal*, pp. 577–582, 2016, doi: 10.1109/ICCA.2016.7505339.
- [5] M. Tampubolon, "Dynamic wireless power transfer for logistic robots," *Energies*, vol. 11, no. 3, p. 527, 2018, doi: https://doi.org/10.3390/en11030527.
- [6] D. Z. & Y. G. Baoping Wang, Qin Sun, "Design of Lithium Battery Management System for Underwater Robot," 10th Int. Conf. Comput. Eng. Networks, vol. 1274, pp. 989–995, 2020, doi: https://doi.org/10.1007/978-981-15-8462-6_113.
- [7] S. L. and D. Sun, "Minimizing energy consumption of wheeled mobile robots via optimal motion planning," *IEEE/ASME Trans. Mechatronics*, vol. 19, no. 2, pp. 401–411, 2014, doi: 10.1109/TMECH.2013.2241777.
- [8] T. W. H. & S. G. Z. Stephen L. Canfield, "Prediction and Experimental Validation of Power Consumption of Skid-Steer Mobile Robots in Manufacturing Environments," J. Intell. Robot. Syst., vol. 94, pp. 825–839, 2019, doi: https://doi.org/10.1007/s10846-018-0779-7.
- [9] W. Y. and C. O. O. Chuy, E. G. Collins, "Power modeling of a skid steered wheeled robotic ground vehicle," *IEEE Int. Conf. Robot. Autom. Kobe, Japan*, pp. 4118–4123, 2009, doi: 10.1109/ROBOT.2009.5152387.
- [10] B. V. and D. L. T. Verstraten, R. Furnémont, G. Mathijssen, "Energy consumption of geared DC motors in dynamic applications: Comparing modeling approaches," *EEE Robot. Autom. Lett.*, vol. 1, no. 1, pp. 524–530, 2016, doi: 10.1109/LRA.2016.2517820.
- [11] Y. N. J. B Lu, L Jan, "Control of cell divisions in the nervous system: symmetry and asymmetry," *Annu Rev Neurosci*, vol. 23, no. 1, pp. 531–56, 2000, doi: 10.1146/annurev.neuro.23.1.531.
- [12] B. C. and R. H. D. MartA-n, "Optimal tuning of a networked linear controller using a multi-objective genetic algorithm," *3rd Int. Conf. Innov. Comput. Inf. Control. Dalian, China*, pp. 91–91, 2008, doi: 10.1109/ICICIC.2008.407.
- [13] P. E. R. et Al, "Enlisting rangers and scouts for reconnaissance and surveillance," *IEEE Robot. Autom. Mag.*, vol. 7, no. 4, pp. 14–24, 2000, doi: 10.1109/100.894029.
- [14] S. S. & J. S. Raymond Sheh, Adam Jacoff, Ann-Marie Virts, Tetsuya Kimura, Johannes Pellenz, "Advancing the state of urban search and rescue robotics through the robocuprescue robot league competition," *F. Serv. Robot.*, vol. 92, pp. 127–142, 2013,



- doi: https://doi.org/10.1007/978-3-642-40686-7_9.
- [15] W. Rizaldy, "INTEGRATION AND TRANSPORTATION OF DANGEROUS GOODS HANDLING MANAGEMENT BETWEEN AIR AND RAILWAY TRANSPORTATION," *Int. J. Res. Commer. Manag. Stud.*, vol. 2, no. 1, pp. 192–207, 2020, [Online]. Available: https://ijrcms.com/uploads2020/ijrcms_02_35.pdf
- [16] N. G. T. and D. G. C. A. Jafari, "A novel intrinsically energy efficient actuator with adjustable stiffness (AwAS)," *IEEE/ASME Trans. Mechatronics*, vol. 8, no. 1, pp. 355–365, 2013, doi: 10.1109/TMECH.2011.2177098.
- [17] K. S. and T. F. K. Wakita, J. Huang, P. Di, "Human-walking-intention-based motion control of an omnidirectional-type cane robot," *IEEE/ASME Trans. Mechatronics*, vol. 18, no. 1, pp. 285–296, 2013, doi: 10.1109/TMECH.2011.2169980.
- [18] T. Y. and F. O. R. Katoh, O. Ichiyama, "A real-time path planning of space manipulator saving consumed energy," *Proc. IECON'94 20th Annu. Conf. IEEE Ind. Electron. Bol. Italy*, vol. 2, pp. 1064–1067, 1994, doi: 10.1109/IECON.1994.397938.
- [19] K.-Y. Tu, "Design of fuzzy potential energy (FPE) for control of a soccer robot," *IEEE Int. Conf. Networking, Sens. Control*, pp. 1105–1109, 2004, doi: 10.1109/ICNSC.2004.1297101.
- [20] C. L. & M. W. M. Jeffrey J. Biesiadecki, "Tradeoffs Between Directed and Autonomous Driving on the Mars Exploration Rovers," *Robot. Res.*, vol. 28, pp. 254–267, 2007, doi: https://doi.org/10.1007/978-3-540-48113-3_23.
- [21] W. H. and N. X. Y. Wu, D. Sun, "Dynamics analysis and motion planning for automated cell transportation with optical tweezers.," *IEEE/ASME Trans. Mechatronics*, vol. 18, no. 2, pp. 706–713, 2013, doi: 10.1109/TMECH.2011.2181856.
- [22] M. W. and Z. S. Tianmiao Wang, Bin Wang, Hongxing Wei, Yunan Cao, "Staying-alive and energy-efficient path planning for mobile robots," *Am. Control Conf. Seattle, WA*, pp. 868–873, 2008, doi: 10.1109/ACC.2008.4586602.
- [23] Y. S. and H.-H. C. J. Chen, J. Li, S. He, "Energy-efficient coverage based on probabilistic sensing model in wireless sensor networks," *IEEE Commun. Lett.*, vol. 14, no. 9, pp. 833–835, 2010, doi: 10.1109/LCOMM.2010.080210.100770.



Copyright © by authors and 50Sea. This work is licensed under Creative Commons Attribution 4.0 International License.